

Structural and rheological characterization of hyaluronic acid-based scaffolds for adipose tissue engineering

Assunta Borzacchiello^{a,*}, Laura Mayol^c, Piera A. Ramires^d, Andrea Pastorello^d,
Chiara Di Bartolo^d, Luigi Ambrosio^a, Evelina Milella^{a,b}

^aIMCB—CNR, P.le Tecchio 80, 80125 Naples, Italy

^bTechnological District on Polymeric and Composite Materials Engineering and Structures—IMAST—P.le E. Fermi 1, Portici-Naples, Italy

^cSchool of Biotechnological Sciences, Department of Pharmaceutical and Toxicological Chemistry, University of Naples Federico II,
Via D. Montesano, 49, 80131 Naples, Italy

^dFidia Advanced Biopolymers, via Ponte della Fabbrica 33/b, 35031 Abano T. (PD), Italy

Received 14 March 2007; accepted 5 June 2007

Available online 28 June 2007

Abstract

In this study the attention has been focused on the ester derivative of hyaluronic acid (HA), HYAFF[®]11, as a potential three-dimensional scaffold in adipose tissue engineering. Different HYAFF[®]11 sponges having different pore sizes, coated or not coated with HA, have been studied from a rheological and morphological point of view in order to correlate their structure to the macroscopic and degradation properties both *in vitro* and *in vivo*, using rat model. The *in vitro* results indicate that the HYAFF[®]11 sponges possess proper structural and mechanical properties to be used as scaffolds for adipose tissue engineering and, among all the analysed samples, uncoated HYAFF[®]11 large-pore sponges showed a longer lasting mechanical stability. From the *in vivo* results, it was observed that the elastic modulus of scaffolds seeded with preadipocytes, the biohybrid constructs, and explanted after 3 months of implantation in autologous rat model are over one order of magnitude higher than the corresponding values for the native tissue. These results could suggest that the implanted scaffolds can be invaded and populated by different cells, not only adipocytes, that can produce new matrix having different properties from that of adipose tissue.

© 2007 Elsevier Ltd. All rights reserved.

Keywords: Adipose tissue engineering; Hyaluronic acid; Scaffold; Viscoelasticity

1. Introduction

Adipose tissue acts as a protective mechanical cushion for tissues and organs such as bones, vessels and nerves. Loss of this tissue can result from congenital malformations, HIV infections, complex traumatic wounds, extensive deep burns, pressure sores and oncologic resections, often causing considerable aesthetic and functional problems. No effective solution for the replacement of adipose tissue has been found. Autologous fat implant undergo shrinkage because of poor vascularization, whereas implants made of synthetic filling biomaterials might induce immune reaction and are rarely integrated by surrounding

tissues [1–4]. Tissue engineering approaches offer considerable potential, but are clearly dependent on the development of appropriate scaffolds.

Recent studies focalized the attention on scaffolds made of synthetic and/or natural polymers, such as poly(lacto-co-glycolic) acid (PLGA) discs or injectable spheres [5,6], polytetrafluorethylene scaffolds [7], collagen gels [8], gelatine microspheres [9] or structures made by reinforcing poly(glycolic acid) fibre-based matrices with poly(L-lactic acid) [10]. Unfortunately, none of these approaches proved to be drawback-free and effective and none of them reached a proper developmental stage for clinical application in humans.

An ideal scaffold for adipose tissue engineering should provide specific biological stimuli, promote vascularization and possess the proper three-dimensional (3D) structure to allow adipose tissue cells to adhere, proliferate and reach

*Corresponding author. Tel.: +39 081 7682104; fax: +39 081 7682404.
E-mail address: bassunta@unina.it (A. Borzacchiello).

a mature phenotype. Since adipocytes are voluminous cells, a spongy 3D structure is believed to be the most adequate scaffold for neo-adipogenesis starting from adipocyte precursors which need space for optimal differentiation. A high degree of porosity and extended specific surface of sponges, in addition, favour the permeability of large quantities of solutions and their homogeneous distribution, which are important features for any engineered construct. Moreover adequate mechanical properties are required for the scaffolds as it should have a sufficient strength to withstand *in vivo* stresses, protect cells from high pressure, being at the same time mechanically biocompatible with the native tissue. Proper scaffold degradation time is also desirable since it should not be resorbed too quickly after transplantation. With respect to scaffold chemical composition, natural derived polymers are believed to favour biocompatibility thanks to their cell interaction capability.

Among the natural materials hyaluronic acid (HA) has long attracted researchers' interest for its unique chemical–physical and biological properties. HA, indeed, is a high-molecular-weight polysaccharide that is a primary component of the extracellular matrix of the connective tissue which regulates and controls several tissue physiological functions *in vivo*. HA contributes to the viscoelastic properties of soft tissues and to their mechanical behaviour in compression [11], and it exerts important functions in joint lubrication, as well [12]. From a biological standpoint, the HA molecule plays a major role in tissue growth and remodelling as it specifically interacts with endogenous receptors such as CD 44, RHAMM, ICAM-1, regulating cellular migration, growth and adhesion [13]. However, the high water affinity strongly limits the use of the native molecule since it leads to poor mechanical properties. Furthermore, the use of unmodified HA as scaffold material for tissue engineering is severely hampered by its poor processability and handling properties. To circumvent these limitations, several approaches have been attempted to chemically modify HA by cross-link or coupling reactions, preserving at the same time its biological activity. A series of derivatives, called HYAFF[®], has been obtained by the esterification of the carboxyl group of the glucuronic acid moiety of the polymer with linear or aromatic alcohol. Among these, the HA benzyl ester, HYAFF[®]11, has been widely used in the biomedical field thanks to its ease of processability and biocompatibility, which has been demonstrated both *in vitro* and *in vivo* [14,15].

HYAFF[®]11 has been clinically used in the form of non-woven felts and films for cartilage and skin tissue engineering [16–19]. HYAFF[®]11, in the form of sponges, was associated to human preadipocytes and the biohybrid constructs were proved to be effective in adipose tissue regeneration in a nude mouse model [20–22]. These studies highlight that scaffolds structure and architecture are key parameters in adipose tissue regeneration and in particular the pore dimension of the sponges was suggested to be crucial for an extensive adipose tissue differentiation in the whole section of the construct.

In this context, the aim of this work was to perform a systematic characterization, by *in vitro* and *in vivo* testing, of different HYAFF[®]11 spongy scaffolds potentially useful in adipose tissue engineering. The scaffold properties were studied by SEM analysis, water absorption tests and rheological characterization. The degradation properties were investigated *in vitro* by monitoring the rheological behaviour and morphological changes as a function of incubation time in cell culture medium; while, *in vivo*, by monitoring the rheological properties of the explanted biohybrid constructs as a function of the implantation times in autologous rat models. The *in vivo* studies play a key role in the understanding of the cell ability to degrade the scaffolds and to produce an extracellular matrix which is mechanically biocompatible with the native tissue.

2. Experimental

2.1. Materials

2.1.1. HYAFF[®]11 sponges

HYAFF[®]11 is a linear derivative of HA obtained by total esterification (>90%) of the carboxyl groups with benzyl alcohol, as previously described [19]. Different HYAFF[®]11 sponge have been supplied by Fidia Advanced Biopolymer (FAB). In particular, sponges with “small” and “large” pore size were obtained using inorganic salts of granulometry of 200–315 and 400–500 µm, respectively. A hydrophilic HA coating was added to the scaffold structure with the main aim to facilitate the process of cell seeding, through a fast medium absorption. HYAFF[®]11-coated sponges were obtained by immersion of HYAFF[®]11 sponges in an aqueous solution of HA biopolymer at a known concentration, and were subsequently freeze-dried. Scaffolds were sterilized by gamma irradiation at 25 Kgy. Sponges produced for this study were characterized by less than 0.2 EU/mg endotoxins and less than 0.1% w/w residual solvents (free benzyl alcohol, ethanol, acetone, DMSO, chloride). HYAFF[®]11 sponges used in this study are summarized in Table 1.

Table 1
Description of HYAFF[®]11 sponges used in this study and their water absorption properties

HYAFF11 sponge type	Granulometry of the salt used in the production process (µm)	Acronym	Water absorption (w/w%)
Small pore	200–315	HY	380 ± 38
Small pore, HA coated	200–315	HYB	1362 ± 15
Large pore	400–500	HYLP	806 ± 140
Large pore, HA coated	400–500	HYBLP	1517 ± 80

Data are means of % absorption of three sponge batches of each type.

2.1.2. Biohybrids construct

Autologous rat preadipocyte were seeded in HYAFF[®]11 large-pore scaffolds, both HA coated and not, by drop-on inoculation method as described elsewhere [21]. After the *in vitro* attachment of preadipocytes to the scaffolds, the resulting biohybrid constructs and a non-seeded scaffold used as control were implanted subcutaneously in two individual pockets in the scapular region of the rat back. From the same animals, native fat tissue was explanted in order to evaluate tissue rheological properties. These scaffolds remained *in vivo* for 3, 8 or 12 weeks. After the indicated time points, rats were sacrificed and the scaffolds were explanted.

2.2. Methods

2.2.1. Water absorption

Water absorption of the different HYAFF[®]11 sponges was determined by adding water to the sponge until the equilibrium was reached and by calculating the weight percentage increase as follows:

$$\% W_{\text{eq}} = \frac{W_s - W_d}{W_d} \times 100,$$

where W_s and W_d are the weight of the sponge at equilibrium and the weight of the dry sponge, respectively.

2.2.2. Rheological properties

The rheological behaviour of HYAFF[®]11 sponges was investigated by dynamic small amplitude shear oscillatory tests by using a rotational rheometer (Gemini, Bohlin Reologi). The tests were performed at controlled temperature of 37 ± 0.1 °C, at the equilibrium swollen state (time = t_0), in culture medium DMEM with 10% (in volume) foetal bovine serum and 2% (in volume) antibiotics.

Preliminary strain sweep tests were performed to evaluate the region of deformation in which the linear viscoelasticity is valid. The oscillatory tests were performed from 0.01 to 10 Hz.

In dynamic experiment, the material is subjected to a sinusoidal shear strain:

$$\gamma = \gamma_0 \sin(\omega t),$$

where γ_0 is the shear strain amplitude, ω the oscillation frequency (which can be also expressed as $2\pi f$ where f is the frequency in Hz) and t the time. The mechanical response, expressed as shear stress τ of viscoelastic materials, is intermediate between an ideal pure elastic solid (obeying to the Hooke's law) and an ideal pure viscous fluid (obeying to the Newton's law) and therefore is out of phase respect to the imposed deformation as expressed by

$$\tau = G'(\omega)\gamma_0 \sin(\omega t) + G''(\omega)\gamma_0 \cos(\omega t),$$

where $G'(\omega)$ is the shear storage modulus and $G''(\omega)$ the shear loss modulus. G' gives information about the elasticity or the energy stored in the material during deformation, whereas G'' describes the viscous character or the energy dissipated as heat.

2.2.3. SEM characterization

HYAFF[®]11 sponges (surface and cross section) were sputter-coated with gold and examined with a scanning electron microscopy (Philips XL 20) at 10 kV acceleration voltage. The sponge cross section was obtained by breaking the sponge after immersion in liquid nitrogen. Image analysis was performed with a software program (NIH Image 1.60, Bethesda, MD, USA) and the sponge morphological features were evidenced by thresholding. Analyses were carried out in an area of about 5 mm² to determine geometrical features of each pore. In particular, the pores area (expressed in μm^2), perimeter (μm) and major and minor diameter of the ellipse with the same gravity center were calculated and used to evaluate the circularity index (C.I.) and the polarity factor. The C.I. was calculated using the following formula: $\text{C.I.} = 4\pi A/P^2$, where A is the pore area and P the pore perimeter. C.I. can range from 1 (a perfect circle) to 0 (a straight line). The 2D polarity factor is defined as the ratio between the lengths of major and

minor axes of an ellipse having the same gravity center; consequently, a circular object would have a polarity factor of unity.

2.2.4. Degradation properties

2.2.4.1. *In vitro*. The *in vitro* degradation properties of the sponges were analysed by monitoring the morphological and rheological changes after incubation in DMEM at different time points. The rheological tests were performed after 1, 3 and 7 days of incubation as previously described. For the morphological properties, SEM analysis was performed after 1 and 7. In this case, the samples were fixed with 2.5% glutaraldehyde in phosphate buffer saline and dehydrated through a grade series of acetone. Then, the sponges were critical point dried (Bal-Tech, Liechtenstein), sputter-coated with gold and examined by SEM, as described above.

2.2.4.2. *In vivo*. Large-pore HYAFF[®]11 sponges loaded with preadipocytes and control sponges (not loaded with cells) were implanted in rat, explanted at fixed time points (3, 8 and 12 weeks) and subjected to rheological analysis as previously described.

3. Results

3.1. Water absorption

Water absorption results are summarized in Table 1. HYAFF[®]11 non-HA-coated sponges with large pores (HYLP) showed double weight percentage increased values than the corresponding sponges with smaller pores (HY) (806 ± 140 vs. $380 \pm 38\%$ w/w, respectively). The HA-coating significantly improved the water absorption ability of the sponges for both small and large pores, minimizing the role of pore sizes on the equilibrium absorbed water amount. Indeed, water absorption values for HA-coated sponges with large- and small-pore sizes was 1517 ± 80 for HYBLP and $1362 \pm 15\%$ w/w for HYB.

3.2. Rheological properties

The mechanical spectra, i.e. the elastic (G') and viscous (G'') moduli as a function of frequency, of the HYAFF[®]11 sponges at t_0 are shown in Fig. 1, while the dynamic modulus values at 1 Hz are reported in Table 2. The rheological behaviour of the sponges is typical of a “strong gel” material, as the viscoelastic moduli, in the frequency range investigated, are quite frequency independent, with an elastic modulus higher than the viscous one of about one order of magnitude. As expected, the values of both viscoelastic parameters are higher for the small-pore sponges than for the large-pore ones, due to the higher presence of void in the latter. In particular, the value of the elastic modulus (G') at the frequency of 1 Hz for the uncoated small-pore sponge is 4.2×10^5 Pa while the corresponding value for the uncoated large-pore sponge is 1.9×10^5 Pa (Table 2). With regard to the HA coating, in the large-pore sponges there is no significant difference among the rheological parameters of the uncoated and coated, indeed the elastic moduli values, at 1 Hz, are respectively 1.9×10^5 and 1.7×10^5 Pa. On the contrary, in the small-pore sponges the HA coating leads to an elastic

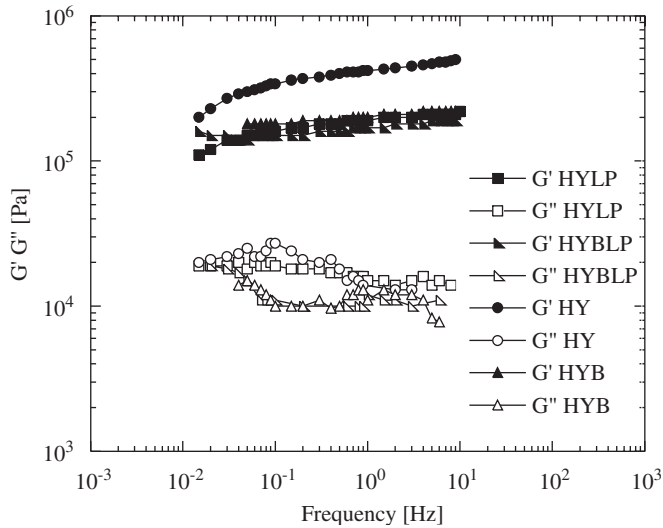


Fig. 1. Dependence of viscous (G'') and elastic (G') moduli upon frequency of HYAFF[®]11 sponges at the equilibrium swollen state in culture medium ($t = 0$) at 37 °C.

modulus reduction of about 50% decreasing, at a frequency equal to 1 Hz, from 4.2×10^5 to 2×10^5 Pa.

3.3. SEM characterization

The surface of the HYAFF[®]11 small-pore sponges (Fig. 2a) is constituted by parallel lamellae with different orientation and a reticulated structure. The large majority of pores on the surface have an area in the range <200 and $500\text{--}1000 \mu\text{m}^2$. The maximum observed diameter is about $100 \mu\text{m}$. In the cross section (Fig. 2b), the peak of distribution of pores area is in the range $1000\text{--}5000 \mu\text{m}^2$ (maximum diameter $200 \mu\text{m}$). The pores localized on the surface are more polarized and oblong than those of the cross section (Fig. 3).

The HA coating modifies the original lamellar structure on the surface of HYAFF[®]11 small-pore sponges (Fig. 2c), making it non-uniform. The majority of pores have an area $<200 \mu\text{m}^2$ (maximum diameter $160 \mu\text{m}$). In the cross section, most of the pores show an area $<500 \mu\text{m}^2$ and

Table 2

Dynamic viscous (G'') and elastic (G') moduli values, at 1 Hz, for all the sponges analysed at different incubation times in culture medium

Viscoelastic moduli (Pa)	t_0	1 day	3 days	7 days
G'_{HYLP}	$1.9e^{+5}$	$1.9e^{+5}$	$2.1e^{+5}$	$1.2e^{+5}$
G'_{HYBLP}	$1.7e^{+5}$	$1.2e^{+5}$	$8.6e^{+4}$	$5.8e^{+4}$
G'_{HY}	$4.2e^{+5}$	$3.3e^{+5}$	$2.7e^{+5}$	$1.7e^{+5}$
G'_{HYB}	$2.0e^{+5}$	$1.9e^{+5}$	$1.5e^{+5}$	$9.6e^{+4}$
G''_{HYLP}	15,000	14,000	16,000	10,000
G''_{HYBLP}	12,000	8700	6300	4400
G''_{HY}	11,000	18,000	15,000	9700
G''_{HYB}	11,000	13,000	10,000	6900

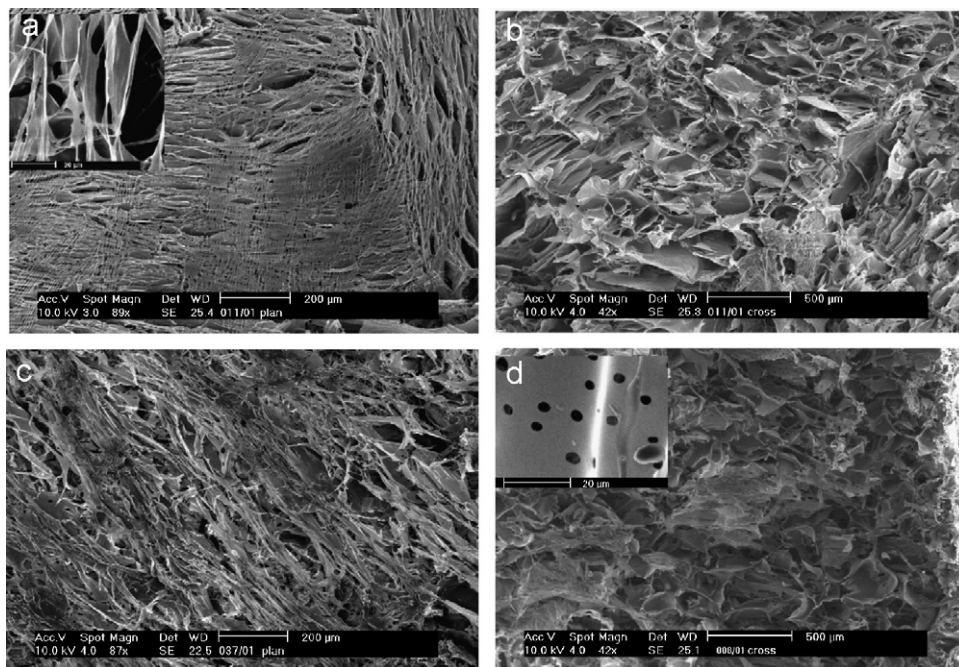


Fig. 2. Scanning electron microscopy images of HYAFF[®]11 small-pore sponges (surface (a) and cross section (b)) and HA-coated HYAFF[®]11 small-pore sponges (surface (c) and cross section (d)). In the panel reported on figures (a) and (d) are indicated some zones with higher magnification.

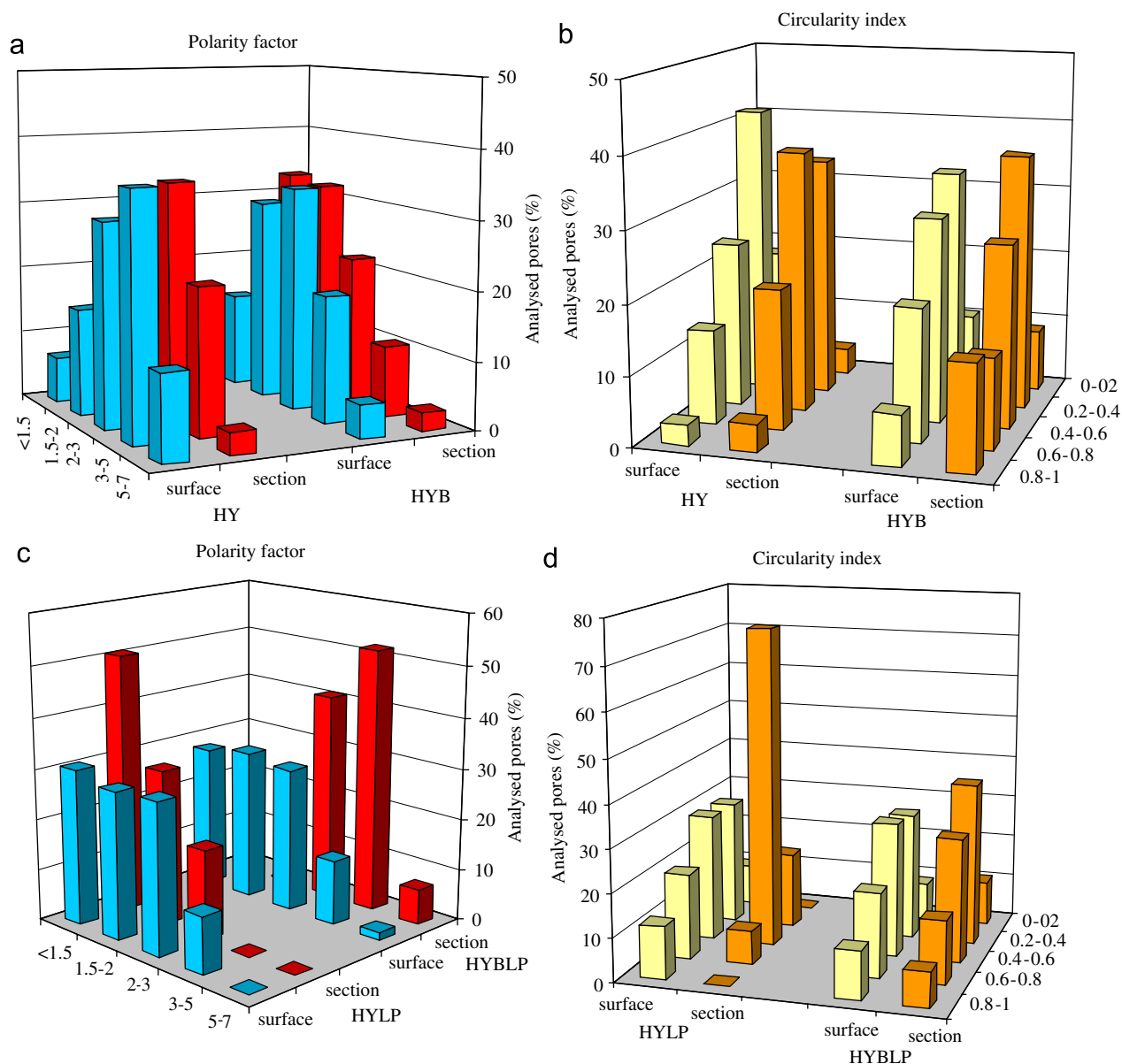


Fig. 3. Polarity factor and circularity index of pores localized on the surface and in the cross section calculated by image analysis of scanning electron microscopy images of HYAFF[®]11 small-pore sponges (a, b) and HYAFF[®]11 large-pore sponges (c, d).

a maximum diameter of 200 μm . The pores localized on the surface are more polarized and oblong than those of the section (Fig. 3). Moreover in the cross section, on the surface of some lamellae, regular pores having small diameter (2–4 μm), round and symmetric shape (C.I. 0.7–0.9; polarity factor 1.1–1.5) are also present.

Generally, the small-pore uncoated sponges have a greater percentage of very polarized (polarity factor 3–5, 5–7) and very oblong pores (0–0.2 and 0.2–0.4) with respect to the coated sponges.

The HYAFF[®]11 large-pore sponge's morphology (Fig. 4) is characterized by large pores both on the surface (up to 0.1 mm^2 , 50–400 μm in diameter) and in the section (up to 0.2 mm^2 , 50–500 μm in diameter). The HA in the

coated sponges modifies the morphology, filling the large pores and in particular making the surface not uniform with parallel and circular structures. The majority of pores on the surface has an area in the range <200 and 500–5000 μm^2 (maximum diameter 200 μm), whereas in the cross section it has an area <5000 μm^2 (maximum diameter 200 μm).

In both coated and uncoated sponges, on the surface there are pores with low asymmetry and polarization (Fig. 3). In the cross section of the uncoated sponges, the pores are little polarized and are on average an average symmetric. On the contrary, in the cross section of HA-coated sponges, the pores with polarized and oblong shape are very numerous.

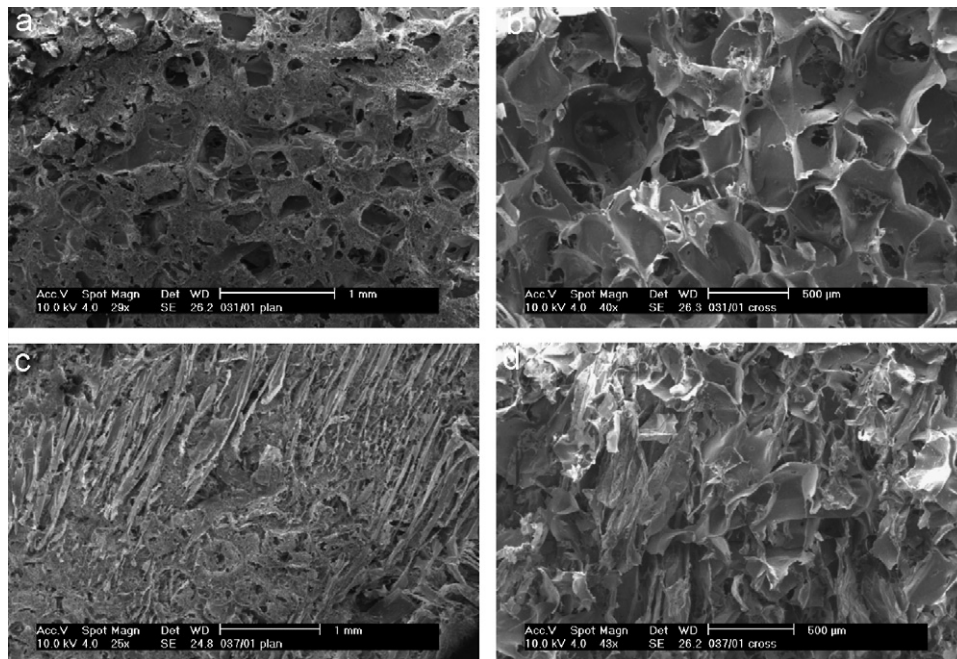


Fig. 4. Scanning electron microscopy images of HYAFF[®]11 large-pore sponges (surface (a) and cross section (b)) and HA-coated HYAFF[®]11 large-pore sponges (surface (c) and cross section (d)).

3.4. Degradation properties

3.4.1. *In vitro*

HYAFF[®]11 dynamic moduli values, at 1 Hz, at different incubation times in culture medium, are reported in Table 2. Both the elastic and viscous moduli decrease as the incubation time increases. The strongest degradation was exhibited by the HA-coated large-pore sponges (HYBLP) whose elastic modulus decreases, after 7 days, of about 66% moving from 1.7×10^5 to 5.8×10^4 Pa. As to the large-pore uncoated sponges (HYLP), G' value passes from 1.9×10^5 to 1.2×10^5 Pa, so exhibiting a reduction of about 37%. Otherwise, the small-pore sponges degradation process seems not to be influenced by the HA covering. Indeed, after 7 days of incubation, the elastic modulus value for HY varies from 4.2×10^5 to 1.7×10^5 Pa and for HYB from 2×10^5 to 9.6×10^4 Pa, thus showing a reduction, respectively, equal to 60% and 52%.

The sponge morphological changes after their incubation in cell culture medium were monitored at 1 and 7 days. The SEM images and the quantitative analyses performed on HYAFF[®]11 small-pore sponges (Fig. 5) showed the formation of small pores ($< 100 \mu\text{m}^2$) on the surface and in the cross section ($< 500 \mu\text{m}^2$) with increasing incubation time (39.3% vs. 26% in surface; 60.6% vs. 35% in cross section). This behaviour is less evident in the HA-coated small-pore sponges. In these sponges, large pores ($> 1000 \mu\text{m}^2$) increased as a function of incubation time (25.6% vs. 19% in surface; 42.4% vs. 35.6% in cross section). Otherwise, HYAFF[®]11 large-pore sponges (Fig. 6) showed an increase of large-pore number ($> 500 \mu\text{m}^2$) on the sample surface and an increase of

small-pore number ($< 500 \mu\text{m}^2$) in the cross section moving from 1 to 7 days of incubation (45.4% vs. 30.6% in surface; 43.8% vs. 32% in cross section). An increase of small-pore number is relevant for HA-coated large-pore sponges, in particular on the surface (38% vs. 23%).

3.4.2. *In vivo*

The elastic modulus as a function of frequency of explanted uncoated scaffolds, HYLP, (control ones, Fig. 7a), and those loaded with cells, the biohybrid, Fig. 7b), at each time point (3, 8 and 12 weeks), is shown and compared to those of the starting scaffolds and native fat in Fig. 7. The elastic modulus values of the control scaffolds and of biohybrid, at a frequency of 1 Hz, for uncoated and coated sponges, are reported, respectively in Fig. 8a and b. The native fat tissue shows “strong gel” mechanical behaviour analogous to that of starting HYAFF[®]11 sponges with viscoelastic moduli values of about two orders of magnitude lower than the corresponding values of the sponges. After implantation, all the HYAFF[®]11 sponges maintain qualitatively the same rheological behaviour, with elastic modulus values higher than the native tissue and lower than the starting scaffolds (Fig. 7). The control elastic modulus decreases with an increase in the implantation time for both HA coated and uncoated sponge as a consequence of HYAFF[®]11 sponges degradation *in vivo* (Fig. 8).

As regards to the biohybrid constructs, for the non-HA-coated sponges, moving from 3 to 8 weeks the elastic modulus value decreases from 18×10^3 to 14×10^3 Pa while, after 12 weeks, its value is slightly higher (about 15×10^3 Pa). Differently, the elastic modulus values of the

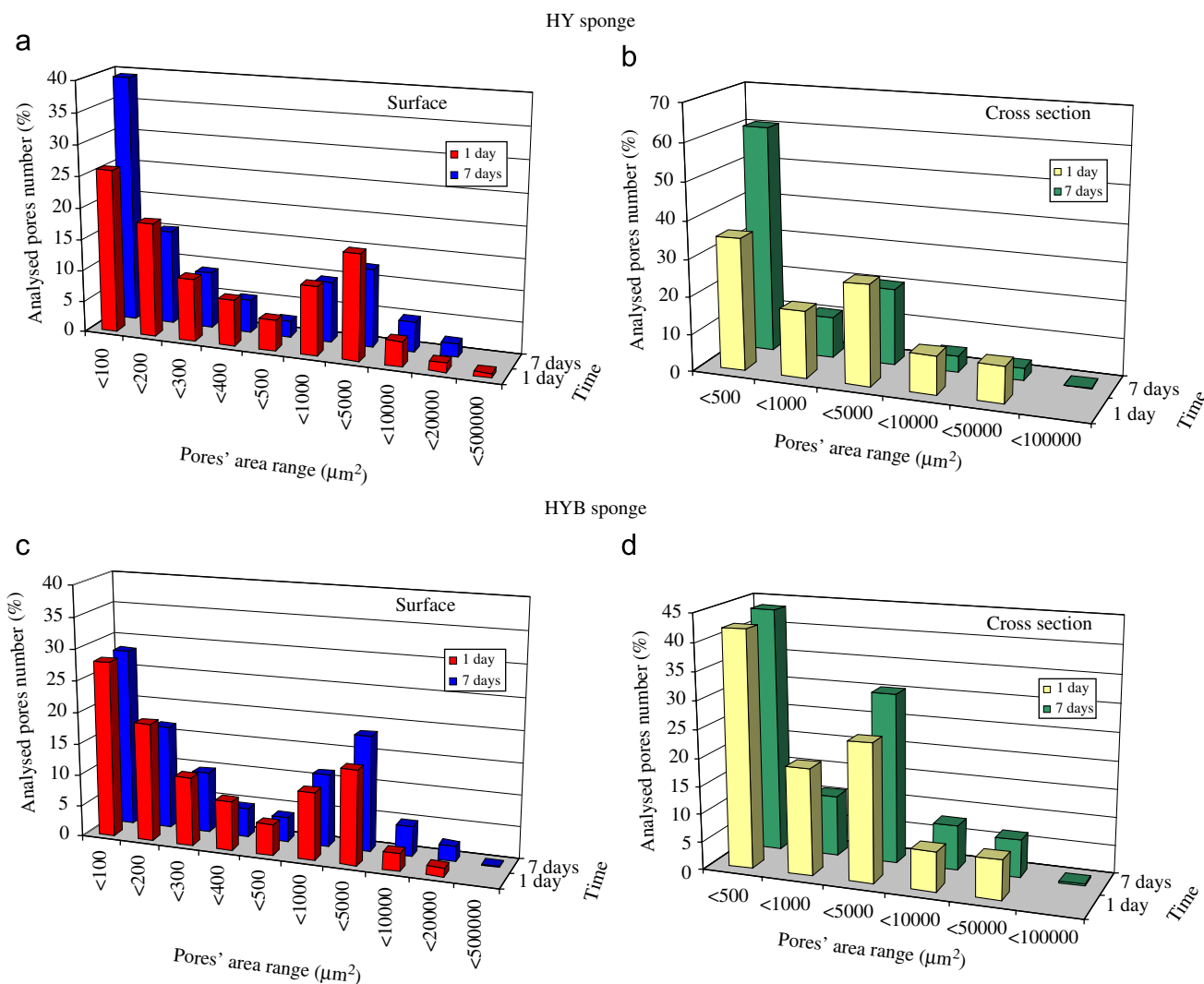


Fig. 5. Percentage of pores number with a determined area calculated by image analysis of scanning electron microscopy images of HYAFF[®]11 small-pore sponges (surface (a) and cross section (b)) and HA-coated HYAFF[®]11 small-pore sponges (surface (c) and cross section (d)) at 1 and 7 days.

coated biohybrid increase with increasing implantation time moving from 9×10^3 to 20×10^3 Pa. Anyway, both the elastic modulus values of coated and uncoated sponges after 12 weeks of implantation remain more than one order of magnitude higher than the corresponding value of native fat tissue (1.5×10^3 Pa).

4. Discussion

In plastic and reconstructive surgery there is a compelling need of adequate solution to the replacement of adipose tissue. A possible solution to soft tissue deficit problems might result from tissue engineering technologies, provided that adequate scaffolds are designed. The biodegradable scaffold must possess specific requirements both in term of material and structure, to allow the cell to differentiate and proliferate. In this work, HA derivatives (HYAFF[®]11) scaffolds, with different pore sizes, HA coated or not, have been studied from a rheological and morphological point of view in order to correlate their

structure to their macroscopic and degradation properties both *in vitro* and *in vivo*.

Qualitatively, the rheological behaviour of all the scaffolds is that typical of a “strong gel” material in which the polymeric chains are cross-linked into a three-dimensional network through physical interactions. Those cross-links among the chains reduce the macromolecular mobility, thus the chain cannot release stress by disentangling and flowing during the period of oscillation and consequently a prevalently elastic behaviour is exhibited. In HYAFF[®]11 sponges, the hydrophobic interactions among the benzyl groups of adjacent chains, together with topological interactions, entanglements and hydrogen bonds existing among the macromolecules, lead to a stable 3D network. As expected, a reduction of about the 50% of the viscoelastic moduli was observed moving from small to large pores for the uncoated samples due to the higher presence of void in the latter.

HYAFF[®]11 small-pore sponges have a morphology characterized by the presence of a lamellar structure, with

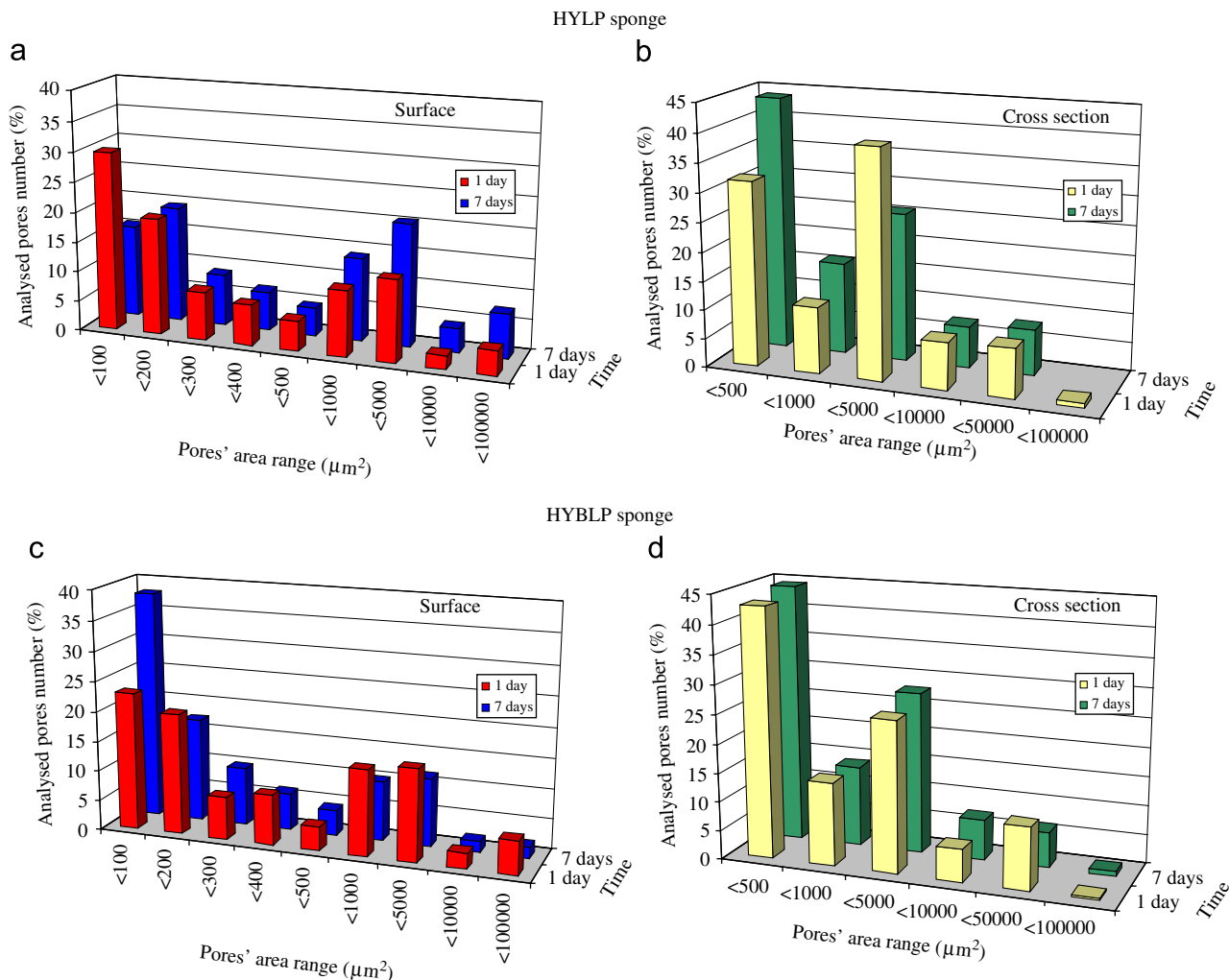


Fig. 6. Percentage of pores number with a determined area calculated by image analysis of scanning electron microscopy images of HYAFF[®]11 large-pore sponges (surface (a) and cross section (b)) and HA-coated HYAFF[®]11 large-pore sponges (surface (c) and cross section (d)) at 1 and 7 days.

very polarized and oblong pores, 48% of which have an area $<200\ \mu\text{m}^2$ (maximum diameter $100\ \mu\text{m}$). On the contrary, the large-pore sponges have a different structure, characterized by a wide distribution in pores' size, including pores with a large area (up to $0.1\ \text{mm}^2$ and $400\ \mu\text{m}$ in diameter). The HA coating considerably affects the sponge morphology producing a significant reduction in pores' area (both in surface and in the cross section). HA coating modifies the parameters of the pores' shape as well. In particular, in the small-pore sponges, HA coating reduces the polarization determining the formation of more symmetric pores. On the contrary, in the cross section of large-pore sponges, HA coating makes the pores more polarized. Due to the pore shape modification induced by the HA coating and to HA hydrophilicity, water absorption is increased in the coated sponges and consequently the plasticizing effect of water leads to a lowering of the sponges mechanical properties. Anyway these sponges have elastic modulus values of the order of magnitude of about $10^5\ \text{Pa}$, showing a proper mechanical stability for cell seeding and for their handling.

Another crucial requirement of a scaffold for tissue engineering is that the substrate should not degrade too quickly after transplantation, keeping mechanical stability to allow a correct extracellular matrix deposition. In this frame, the sponge's degradation properties were investigated using both an *in vitro* and an *in vivo* model. As for the *in vitro* experiments, the sponge's rheological behaviour and morphological changes were monitored as a function of incubation time in cell culture medium while, for the *in vivo* tests, biohybrid constructs rheological properties changes were monitored as a function of the implantation times in autologous rat models. Generally, when incubated in a culture medium the sponges undergo a change in their original morphology. In the small-pore sponges, with increasing incubation time, an increase of the small-pore percentage occurs both in surface and cross section. In the presence of the HA coating, the pores with a large area increase as well. In the large-pore sponges, an increase of pores' area occurs only on the surface, whereas in the cross section the behaviour is comparable to the small sponges. The presence of HA coating produces an increase in pores'

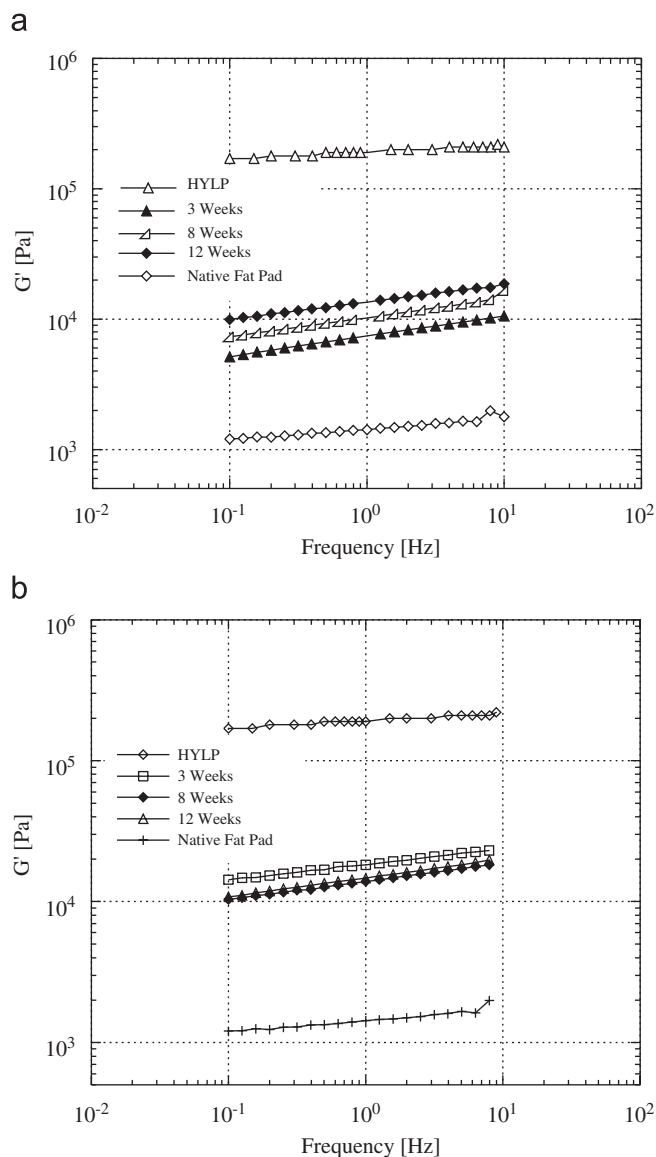


Fig. 7. (a, b) Dependence of elastic (G') modulus upon frequency, at different time points, of non-HA-coated HYAFF[®]11 control sponges (a) and non-HA-coated biohybrid constructs (b).

percentage with small area on the samples surface and a slight increase of pores with large area in the cross section.

Consistently with the morphological observations, the mechanical results show a reduction of the sponge's elastic modulus and, in particular, for HYBLP of about the 67%, for HYL P 37%, for HY 60% and for HYB 50%. This indicates a degradation of the total benzyl ester sponges which is due to a hydrolytic breakdown [20] of the polymer chains and so a progressive rupture of the three-dimensional network responsible of its rheological behaviour. The HYAFF[®]11-uncoated large-pore sponges preserve a longer lasting mechanical stability compared to all kind of the analysed sponges. The proper performances of HYAFF[®]11 large-pore scaffolds have been also remarked in an *in vitro* study [21] in which the highest preadipocytes attachment rate was observed for large-pore

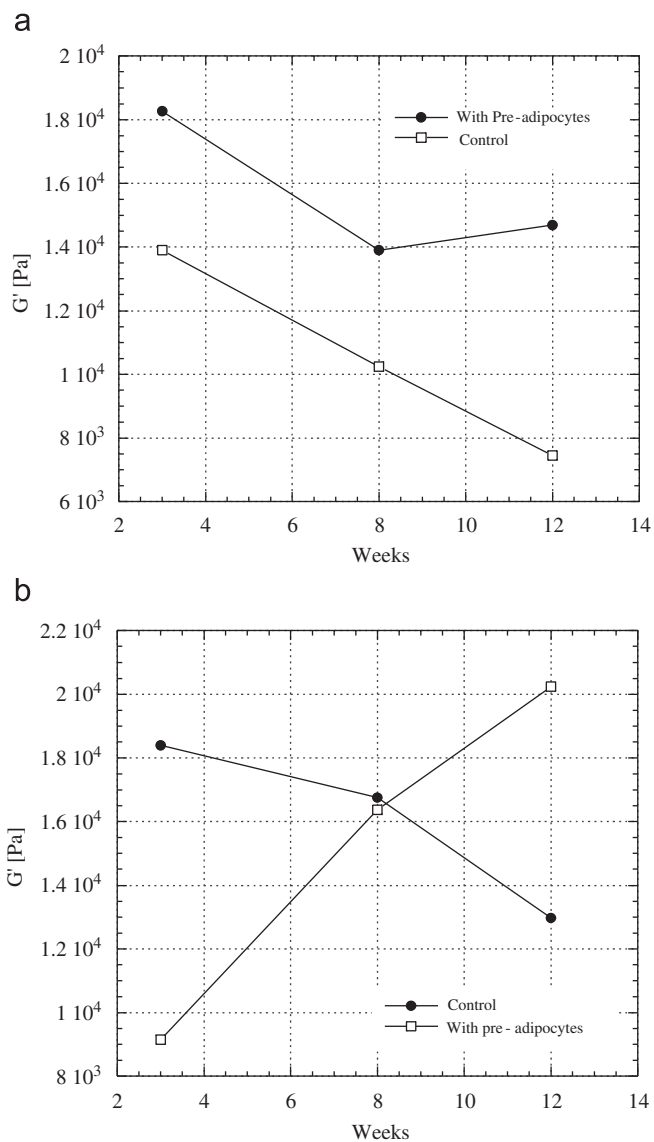


Fig. 8. (a, b) Dependence of elastic (G') modulus at 1 Hz upon implantation time of HYAFF[®]11 control sponges and biohybrid constructs non-HA-coated (a) and HA-coated (b).

sponges. According to these results, the degradation properties *in vivo* were studied only on the large-pore sponge HA coated and not. The elastic modulus value of the control scaffolds (not loaded with cells) decreases with increasing implantation time both for HYBLP and HYL P as a consequence of HYAFF[®]11 sponge degradation *in vivo*.

As regards to the biohybrid constructs, for the non-HA-coated sponges, the elastic modulus value first decreases and then slightly increases from 3 to 8 and to 12 weeks. Differently, the elastic modulus values of the coated biohybrids always increase with increasing implantation time. For both the coated and uncoated sponges, anyway, the elastic modulus of the biohybrids after 3 months of implantation remains well over one order of magnitude higher than the corresponding value for the native tissue. These results could suggest that the implanted scaffolds can

be invaded and populated by different cells, not only adipocytes, that can produce new matrix, such as fibrous tissue, having different properties from that of adipose tissue. These results are in agreement with a recent *in vivo* study, in which HYAFF[®]11 HA-coated and uncoated large-pore sponges, loaded with preadipocyte, were implanted in the nude mouse. Even if a better penetration of cells was observed with respect to the small-pore sponges, no mature adipocyte were found in the sponges after explantation. Moreover, histological and immunohistological examination of the scaffolds revealed predominantly fibrous tissue separating and surrounding the sponge material [22]. As a consequence, we can conclude that even if the HYAFF[®]11 uncoated large-pore sponges present structural, rheological and degradation properties suitable for application as scaffolds for adipose tissue engineering, they need to be further optimized from a biological point of view.

5. Conclusion

Different HYAFF[®]11 sponges, potentially useful in adipose tissue engineering, having different pore sizes, coated with HA or not, have been characterized by *in vitro* and *in vivo* testing. The rheological and morphological properties, as well as the *in vitro* degradation behaviour of the scaffolds are strongly influenced by the coating and by the pores dimensions. These sponges have elastic modulus values of the order of magnitude of about 10^5 Pa, showing a proper mechanical stability for cell seeding and for their handling. From the *in vivo* tests it was observed that the elastic modulus of the scaffold seeded with preadipocyte after 3 months of implantations, in autologous rat model, remains over one order of magnitude higher than the corresponding value for the native tissue, suggesting that the implanted scaffolds can be invaded and populated by different cells, not only adipocytes, that can produce new matrix different from adipose tissue.

Acknowledgements

The authors would like to thank EC for financial support (EC-Funded Project No. GRD1—1999-11159).

References

- [1] Henriksen TF, Holmich LR, Fryzek JP, Friis S, McLaughlin JK, Hoyer AP, et al. Incidence and severity of short term complications after breast augmentation: results from a nationwide breast implant registry. *Ann Plast Surg* 2003;51:531–9.
- [2] Siggelkow W, Klosterhalfen B, Klinge U, Rath W, Faridi A. Analysis of local complications following explantation of silicone breast implants. *Breast* 2004;13:122–8.
- [3] Klein AW, Rish DC. Substances for soft tissue augmentation: collagen and silicone. *J Dermatol Surg Oncol* 1985;11:337–9.
- [4] Hartrampf CR, Schean M, Black PW. Breast reconstruction with a transverse abdominal island. *Plast Reconstr Surg* 1982;69:216–25.
- [5] Patrick CW, Chauvin PB, Hobley J, Reece GP. Preadipocyte seeded PLGA scaffolds for adipose tissue engineering. *Tissue Eng* 1999;2: 139–51.
- [6] Choi YS, Park SN, Suh H. Adipose tissue engineering using mesenchymal stem cells attached to injectable PLGA spheres. *Biomaterials* 2005;26:5855–63.
- [7] Kral JG, Crandall DL. Development of a human adipocyte synthetic polymer scaffold. *Plast reconstr Surg* 1999;104:1732–8.
- [8] Huss FR, Kratz G. Mammary epithelial cell and adipocyte coculture in a 3-D matrix: the first step towards tissue-engineered human breast tissue. *Cells Tissues Organs* 2001;169:361–7.
- [9] Kimura Y, Ozeki M, Inamoto T, Tabata Y. Adipose tissue engineering based on human preadipocytes combined with gelatin microspheres containing basic fibroblast growth factor. *Biomaterials* 2003;24:2513–21.
- [10] Cho S-W, Kim S-S, Rhie JW, Cho HM, Cho CY, Kim B-S. Engineering of volume-stable adipose tissues. *Biomaterials* 2005;26: 3577–85.
- [11] Mow VC, Holmes MH, Lai WM. *J Biomech* 1984;17:377.
- [12] Ambrosio L, Borzacchiello A, Netti PA, Nicolais L. *J Macromol Sci Pure Appl Chem* 1999;A36:991.
- [13] Agren U, Tolg C, Paiwand F, Paiwand SA, Turkeley SA, Harrison R, et al. In: Abatangelo G, Weigel PH, editors. *New frontiers in medical sciences: redefining Hyaluronan*. Amsterdam: Elsevier Science; 2000. p. 63.
- [14] Cortivo R, Brun P, Rastrelli A, Abatangelo G. *In vitro* studies on biocompatibility of hyaluronic acid esters. *Biomaterials* 1991;12: 727–30.
- [15] Benedetti L, Cortivo R, Berti T, Pea F, Mazzo M, Moras M, et al. Biocompatibility and biodegradation of different hyaluronan derivatives (HYAFF) implanted in rats. *Biomaterials* 1993;14(15): 1154–60.
- [16] Campoccia D, Doherty P, Radice M, Brun P, Abatangelo G, Williams D. Semisynthetic resorbable materials from hyaluronan esterification. *Biomaterials* 1998;19:2101–17.
- [17] Solchaga LA, Goldberg VM, Caplan AI. Hyaluronic acid-based biomaterials in tissue engineered cartilage repair. In: Abatangelo G, Weigel PH, editors. *Redefining hyaluronan*. Amsterdam, The Netherlands: Elsevier Science B.V.; 2000. p. 233–46.
- [18] Caravaggi C, et al. Hyaff11-based Autologous dermal and epidermal grafts in the treatment of noninfected diabetic plantar and dorsal foot ulcers. A prospective, multicenter, controlled, randomized clinical trial. *Diabetes Care* 2003;26(10):2853–9.
- [19] Milella E, Brescia E, Massaro C, Ramires PA, Miglietta MR, Fiori V, et al. Physico-chemical properties on degradability of non-woven hyaluronan benzylic ester as tissue engineering scaffolds. *Biomaterials* 2002;23(4):1053–63.
- [20] von Heimburg D, Zachariah S, Low A, Pallua N. Influence of different biodegradable carriers on the *in vivo* behavior of human adipose precursor cells. *Plast Reconstr Surg* 2001;108:411–20.
- [21] Halbleib M, Skurk T, de Luca C, von Heimburg D, Hauner H. Tissue engineering of white adipose tissue using hyaluronic acid-based scaffolds. I: *in vitro* differentiation of human adipocyte precursor cells on scaffolds. *Biomaterials* 2003;24:3125–32.
- [22] Hemmrich K, von Heimburg D, Rendchen R, Di Bartolo C, Milella E, Pallua N. Implantation of preadipocyte-loaded hyaluronic acid-based scaffolds into nude mice to evaluate potential for soft tissue engineering. *Biomaterials* 2005;26(34):7025–37.